Oscillating Streaming Potential and Electro-osmosis of Multilayer Membranes

Jun Yang,[†] Karina Grundke,[‡] Cornelia Bellmann,[‡] Stefan Michel,[‡] Larry W. Kostiuk,[†] and Daniel Y. Kwok*[,†]

Department of Mechanical Engineering, University of Alberta, Edmonton, Alberta, T6G 2G8, Canada T6G, and Institute of Polymer Research, Dresden, Hohe Strausse 6, D-01069, Dresden, Germany

Received: July 7, 2003; In Final Form: November 21, 2003

Artificial membranes consist of multilayers that have different physical or chemical properties. They are often considered as an equivalent single-layer membrane without taking into account the detail inside. Based on the Debye−Hückel approximation, we have provided analytical solutions of oscillating electrokinetic flow in multilayer membranes. Both pressure-driven flow (streaming potential) and electric-field-driven flow (electro-osmosis) were studied. The pressure and electric-field distributions in each layer can be obtained from our analytical solutions. This allows a better understanding of electrokinetic flow in multilayer membranes and benefits the design and selection of artificial membranes. The derived analytical solutions are useful for more-general time-dependent problems through a superposition of time-harmonic solutions weighted by appropriate Fourier coefficients. The properties of each membrane layer are reflected as complex quantities; therefore, a method is proposed to determine the electrokinetic properties (such as the zeta potential) of each layer by applying a high-frequency alternating electric field or pressure.

I. Introduction

Because of the requirement of mechanical strength, multilayer membranes with graded chemical, physical, and mechanical properties are widely used in filtration, desalination, and separation processes.[1] However, the characterization of the electrochemical properties of multilayer membranes, such as zeta potential, is typically based on any given electrokinetic model through streaming potential[2−6] or electro-osmosis[7−11] measurements. A more-detailed description of the zeta potential and the electrical double layer can be found elsewhere.[12−16] Note that the traditional electrokinetic model[17−19] does not consider the detailed multilayer structure; hence, the measured zeta potential can only be called the "apparent zeta potential". Obviously, a single apparent zeta potential could not fully describe the electrokinetic properties of multilayer membranes. On the other hand, electrokinetic transport phenomena in multilayer membranes are complex, because of their heterogeneous porosities and the variation of pore sizes and zeta potentials for each layer. It is, therefore, important to study the nature of electrokinetic flow inside each layer. It would also be of interest to characterize the role of each layer on electrokinetic flow. Thus, there is a need to develop a detailed model to determine its electrokinetic property and flow behavior inside a multilayer membrane. Furthermore, a fundamental understanding of electrokinetic flow in multilayer membranes also provides guidelines for the design and characterization of multilayer membranes.

The first step in this topic has been performed by Szymczyk and co-workers.[20,21] For membranes with two or three layers, they theoretically established a relationship between the global streaming potential of multilayer membranes and that of individual layers. Good agreement was obtained between the experimental data and those from theoretical considerations. In the case of streaming potential, we extend their work here and provide a more-general solution for the velocity, pressure, electric-field distribution, current, and flow rate in each layer of a multilayer membrane. In addition, electro-osmosis is also a popular method to determine the zeta potential of a membrane.[7−11] Because of the flow rate and current continuity requirements, pressure gradients are induced inside each layer during electro-osmosis, and it is necessary to understand the pressure distribution inside a multilayer membrane. Thus, we also extend our model to describe electro-osmosis (electric-field-driven flow). An alternating electric or time-dependent pressure field can be used to characterize such membranes;[22] therefore, we have expressed our oscillating solutions for more-general time-dependent problems through a superposition of time-harmonic solutions weighted by the appropriate Fourier coefficients. A formula for performing the zeta potential measurements of multilayer membranes by streaming potential or electro-osmosis measurements is also proposed. We find that the oscillating responses of multilayer membranes could allow determination of all features of each layer. Changing the frequency of oscillations as input, one would have enough information to solve for all properties for each layer. A nondestructive frequency determination method for zeta potentials could also be developed for unknown multilayer membranes.

II. Controlling Equations and Boundary Conditions in an Individual Pore

For a multilayer membrane with N layers (Figure 1), we assume the pores in any given layer to be uniform with the same property. For an individual pore in the mth layer, we consider a boundary value problem for oscillating electrolyte flow driven by an oscillating pressure gradient and electric field. A local cylindrical coordinate system (r,θ,z) is used, where the z-axis is taken to coincide with the central axis of the pore. All

* Author to whom correspondence should be addressed. E-mail: daniel.y.kwok@ualberta.ca.
† University of Alberta.
‡ Institute of Polymer Research, Dresden.

10.1021/jp0359485 CCC: $27.50
Published on Web 01/16/2004

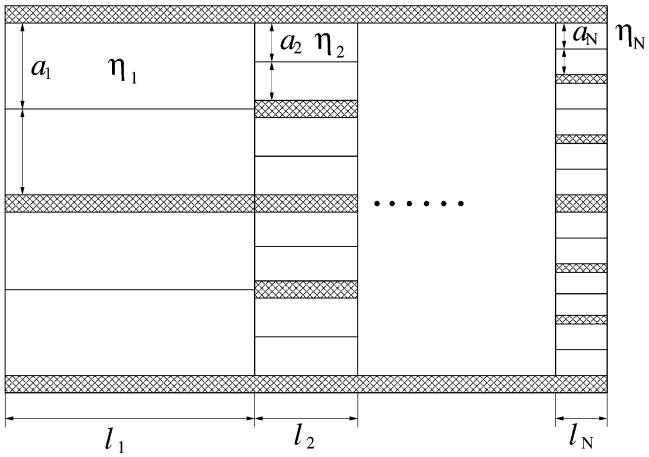

Figure 1. Schematic of a multilayer membrane.

field quantities are assumed to be dependent on the radial coordinate r and time t. The boundary value problem, with the relevant field equations and boundary conditions, are shown below.

A. Electrical Field. Each layer has its own physical and chemical properties; therefore, the electrical double layer in each layer would have its own zeta potential and ion distribution. The permittivity of solution in the electrical double layer for each layer is also different, which causes differences in the electric field. For simplicity, we only consider the deviation of electric field strength. The total potential U_m of the mth layer at location (r,z) at a given time t (the subscript m denotes properties for the mth layer) is taken to be

$$U_m \equiv U_m(r,z,t) = \psi_m(r) + [U_{0,m} - zE'_{z,m}(t)] \qquad (1)$$

where $\psi_m(r)$ is the potential due to the double layer at the equilibrium state (i.e., no liquid motion with no applied external field), $U_{0,m}$ is the potential at the beginning of the mth layer $z = 0$ (i.e., $U_{0,m} \equiv U_m(r,0,t)$), and $E'_{z,m}(t)$ is the spatially uniform time-dependent electric-field strength in the mth layer. The total potential U_m in eq 1 is axisymmetric and, when $E'_{z,m}(t)$ is time-independent, eq 1 is similar to eq 6.1 in the work of Masliyah.[23] The time-dependent flow to be studied here is assumed to be sufficiently slow such that the radial charge distribution is relaxed at its steady state. Furthermore, it is assumed that any induced magnetic fields are sufficiently small and negligible, such that the total electric field may still be defined as $-\nabla U_m$;[24] this definition may then be used to obtain the Poisson equation,

$$\nabla^2 U_m = -\frac{\rho_m}{\epsilon} \qquad (2)$$

where ρ_m is the free charge density and ϵ is the permittivity of the medium. Combining eqs 1 and 2 yields the following Poisson equation (in cylindrical coordinates):

$$\frac{1}{r}\frac{d}{dr}\left(r\frac{d\psi_m(r)}{dr}\right) = -\frac{\rho_m}{\epsilon} \qquad (3)$$

The conditions imposed on $\psi_m(r)$ are

$$\psi_m(a_m) = \zeta_m \qquad (\psi_m(0) \text{ is finite}) \qquad (4)$$

where ζ_m is the zeta potential near the pore wall in the mth layer, with $r = a_m$. For brevity, we shall focus on a symmetric, binary electrolyte with univalent charges. The cations and anions are identified as species 1 and 2, respectively. Based on the assumption of thermodynamic equilibrium, the Boltzmann equation provides a local charge density $\rho_{i,m}$ of the ith species. Thus,

$$\rho_{i,m} = z_i e n_\infty \exp\left[-\frac{z_i e \psi_m}{kT}\right] \qquad (\text{for } i = 1, 2) \qquad (5)$$

where z_i is the valence of the ith species, e the elementary charge; n_∞ the ionic concentration in an equilibrium electrochemical solution at the neutral state (where $\psi_m = 0$ or is so small that it can be neglected), k the Boltzmann constant, and T the absolute temperature. Invoking the Debye−Hückel approximation for low zeta potentials ($z_i e\psi/(kT) \ll 1$), which provides an acceptable prediction, even when the zeta potential is as large as 100 mV,[25] we could solve the Poisson−Boltzmann equation with an analytical solution. Numerical integration of the Poisson−Boltzmann equation can be found elsewhere.[26,27] With the approximation, we express $\sinh[z_0 e\psi_m/(kT)] \approx z_0 e\psi_m/(kT)$ and the total charge density follows from eqs 3 and 5 as

$$\rho_m = \sum_{i=1}^{2} \rho_{i,m} = \left(\frac{-2n_\infty e^2 z_0^2}{kT}\right)\psi_m \qquad (6)$$

where we have used $z_1 = -z_2 = z_0$. Finally, the definition of the reciprocal of the double-layer thickness for a $(z_0{:}z_0)$ electrolyte is given as

$$\kappa = \sqrt{\frac{2n_\infty e^2 z_0^2}{\epsilon kT}} \qquad (7)$$

Combining eqs 3 and 6 results in

$$\frac{1}{r}\frac{d}{dr}\left(r\frac{d\psi_m(r)}{dr}\right) = \kappa^2\psi_m$$
$$\psi(a_m) = \zeta_m \qquad (8a)$$

and

$$\frac{\partial\psi_m(0)}{\partial r} = 0 \qquad (8b)$$

where a is the radius of the pores.

B. Hydrodynamic Field. The axial electric field will induce a body force $\rho_m E'_{z,m}$ and the modified Navier−Stokes equation becomes

$$-\frac{1}{\mu}\frac{\partial p_m}{\partial z} + \frac{1}{r}\frac{\partial}{\partial r}\left(r\frac{\partial v_m}{\partial r}\right) + \frac{1}{\mu}\rho_m E'_{z,m} = \frac{1}{\nu}\frac{\partial v_m}{\partial t} \qquad (9)$$

where we have taken the pressure gradient $[(\partial p/\partial z) \equiv (\partial p/\partial z)(t)]$ to be position-independent, μ is the viscosity, and ν is the kinematic viscosity of the liquid. The boundary conditions for the velocity field are

$$v_m(a_m,t) = 0 \qquad (10a)$$

and

$$\frac{\partial v_m(0,t)}{\partial r} = 0 \qquad (10b)$$

The electric current density along the pore may be integrated over the channel cross section to give the electric current:

$$I_m = 2\pi\int_0^{a_m}\rho_m v_m r\,\mathrm{d}r + \pi a_m^2\lambda E'_{z,m} \tag{11}$$

where λ is the conductivity of bulk electrolyte. Note that, for multilayer membranes, the solution in each layer might have different conductivities, because of the difference in pore sizes. This effect is more noticeable when the concentration of electrolyte solution is low, which causes a larger contribution of surface conductivity to the total conductivity.[6,28] In eq 11, the first term on the right-hand side is due to bulk convection and the second term is attributed to conduction current. The flow rate (Q_m) can be written as

$$Q_m = 2\pi\int_0^{a_m} v_m r\,\mathrm{d}r \tag{12}$$

III. Analytical Solution for an Individual Pore

Here, an analytical solution is sought for a sinusoidal periodicity in the electrohydrodynamic fields, and this is best addressed through the use of complex variables. Thus, a general field quantity X may be defined as the real part of the complex function $X^*e^{j\omega t}$, where X^* is complex ($j = \sqrt{-1}$), ω the oscillation frequency, and t the time. The general field quantity X is written as

$$X = \mathrm{Re}[X^*e^{j\omega t}] \tag{13}$$

The phase angle (ϕ) is defined as

$$\phi = \tan^{-1}\frac{\mathrm{Im}(X^*)}{\mathrm{Re}(X^*)} \tag{14}$$

where $\mathrm{Im}(X^*)$ and $\mathrm{Re}(X^*)$ are the imaginary and real parts of X^*, respectively. An alternative representation of eq 13 is given as

$$X = \mathrm{Re}[|X^*|e^{j(\omega t+\phi)}] \tag{15}$$

where

$$|X| = |X^*| \tag{16a}$$

and

$$|X^*| = \sqrt{\mathrm{Im}^2(X^*) + \mathrm{Re}^2(X^*)} \tag{16b}$$

With the notation of eq 13, we shall seek the solution of the boundary value problem for the following specific dependencies:

$$-\frac{\partial p_m}{\partial z} = \mathrm{Re}[P^*_m e^{j\omega t}]$$

$$E'_{z,m} = \mathrm{Re}[E^*_{z,m}e^{j\omega t}] \tag{17}$$

We consider the class of solutions where the amplitude of the pressure gradient (P^*) and the electric field (E^*_z) could be frequency-dependent, i.e., $P^*_m \equiv P^*_m(\omega)$ and $E^*_{z,m} \equiv E^*_{z,m}(\omega)$. The solution for ψ_m will then follow from eq 8, and that for v_m will follow from eq 9. Thus,

$$v_m = \mathrm{Re}[v^*_m e^{j\omega t}]$$

where

$$v^*_m \equiv v^*_m(r,\omega) = v^*_{p,m}(r,\omega)P^*_m(\omega) + v^*_{E,m}(r,\omega)E^*_{z,m}(\omega) \tag{18}$$

The expression for $v^*_{p,m}(r,\omega)$ and $v^*_{E,m}(r,\omega)$ will be given at the end of this section. The electric current will follow from eq 11 and may be written as

$$I_m = \mathrm{Re}[I^*_m e^{j\omega t}]$$

where

$$I^*_m \equiv I^*_m(\omega) = I^*_{p,m}(\omega)P^*_m(\omega) + I^*_{E,m}(\omega)E^*_{z,m}(\omega) \tag{19}$$

The volumetric flow rate Q_m (defined in eq 12) becomes

$$Q_m = \mathrm{Re}[Q^*_m e^{j\omega t}]$$

where

$$Q^*_m \equiv Q^*_m(\omega) = Q^*_{p,m}(\omega)P^*_m(\omega) + Q^*_{E,m}(\omega)E^*_{z,m}(\omega) \tag{20}$$

During pressure-driven flow, the amplitude of the electric-field strength of streaming potential $E^*_{z,m}(\omega)$ is found by setting $I^* = 0$ in eq 19. Thus,

$$E^*_{z,m}(\omega) = -\frac{I^*_{p,m}(\omega)}{I^*_{E,m}(\omega)}P^*_m(\omega) \qquad (\text{for } I^*_m = 0) \tag{21}$$

Equation 21 may be substituted into eqs 18 and 20 to determine the normalized liquid velocity and volumetric flow rate, respectively. Alternatively, the velocity, current, and volumetric flow rate during electro-osmotic flow follow from eqs 18−20 by setting $P^*_m(\omega) = 0$.

The velocity, current, and flow rate of an individual pore in eqs 18−20 are listed below.

$$v^*_{p,m}(r,\omega) = \frac{1}{j\omega\rho_d}\left[1 - \frac{J_0\left(r\sqrt{\frac{-j\omega}{\nu}}\right)}{J_0\left(a_m\sqrt{\frac{-j\omega}{\nu}}\right)}\right] \tag{22}$$

$$v^*_{E,m}(r,\omega) = \frac{\epsilon\kappa^2\zeta_m}{(\kappa^2\nu - j\omega)\rho_d}\left[\frac{J_0(j\kappa r)}{J_0(j\kappa a_m)} - \frac{J_0\left(r\sqrt{\frac{-j\omega}{\nu}}\right)}{J_0\left(a_m\sqrt{\frac{-j\omega}{\nu}}\right)}\right] \tag{23}$$

$$I^*_{p,m}(\omega) = \frac{2\pi\epsilon\kappa^2\zeta_m}{\rho_d}\left\{\frac{a_m J_1(j\kappa a_m)}{\omega\kappa J_0(j\kappa a_m)} - \frac{\nu a_m}{\omega^2 + j\omega\kappa^2\nu}\left[j\kappa\frac{J_1(j\kappa a_m)}{J_0(j\kappa a_m)} - \sqrt{\frac{-j\omega}{\nu}}\frac{J_1\left(a_m\sqrt{\frac{-j\omega}{\nu}}\right)}{J_0\left(a_m\sqrt{\frac{-j\omega}{\nu}}\right)}\right]\right\} \tag{24}$$

$$I^*_{E,m}(\omega) = \frac{-2\pi\epsilon^2\kappa^4\zeta_m^2}{(\kappa^2\nu - j\omega)\rho_d}\left\{\frac{a_m^2}{2}\left[1 + \frac{J_1^2(j\kappa a_m)}{J_0^2(j\kappa a_m)}\right] - \frac{\nu a_m}{j\omega - \kappa^2\nu}\times\left[j\kappa\frac{J_1(j\kappa a_m)}{J_0(j\kappa a_m)} - \sqrt{\frac{-j\omega}{\nu}}\frac{J_1\left(a_m\sqrt{\frac{-j\omega}{\nu}}\right)}{J_0\left(a_m\sqrt{\frac{-j\omega}{\nu}}\right)}\right]\right\} + \pi a_m^2\lambda_m \tag{25}$$

$$Q^*_{p,m}(\omega) = \frac{2\pi}{j\omega\rho_d}\left\{\frac{a_m^2}{2} - \frac{a_m}{\sqrt{\frac{-j\omega}{\nu}}}\left[\frac{J_1\left(a_m\sqrt{\frac{-j\omega}{\nu}}\right)}{J_0\left(a_m\sqrt{\frac{-j\omega}{\nu}}\right)}\right]\right\} \quad (26)$$

$$Q^*_{E,m}(\omega) = \frac{2\pi\epsilon\kappa^2\zeta_m}{(\kappa^2\nu - j\omega)\rho_d}\left\{\frac{a_m J_1(j\kappa a_m)}{j\kappa\ J_0(j\kappa a)} - \frac{a_m}{\sqrt{\frac{-j\omega}{\nu}}}\left[\frac{J_1\left(a_m\sqrt{\frac{-j\omega}{\nu}}\right)}{J_0\left(a_m\sqrt{\frac{-j\omega}{\nu}}\right)}\right]\right\} = I^*_{p,m}(\omega) \quad (27)$$

where J_0 and J_1 are the zeroth- and first-order Bessel functions of the first kind, ρ_d is the liquid density, and ν is the kinematic viscosity. Here, we find that $Q^*_{E,m} = I^*_{p,m}$ satisfies Onsager's theorem.[29] Normally, we define the streaming current ($I_{str,m}$) as the first term of eq 11, or $I_{str,m} = \mathrm{Re}[(I^*_{p,m}P^*_m + I^*_{E,m}E^*_{z,m} - \pi a_m^2\lambda_0 E^*_{z,m})e^{j\omega t}]$.

When $\omega \to 0$, eqs 22−27 reduces to those of steady state.

$$v^*_{p,m}(r,0) = \frac{1}{4\nu\rho_d}(a_m^2 - r^2) \quad (28a)$$

$$v^*_{E,m}(r,0) = -\frac{\epsilon\zeta_m}{\nu\rho_d}\left[1 - \frac{J_0(j\kappa r)}{J_0(j\kappa a_m)}\right] \quad (28b)$$

$$I^*_{p,m}(0) = -\frac{\epsilon\zeta_m\pi a^2}{\nu\rho_d}\left[1 - \frac{2}{j\kappa a_m}\frac{J_1(j\kappa a_m)}{J_0(j\kappa a_m)}\right] \quad (28c)$$

$$I^*_{E,m}(0) = -\frac{\epsilon^2\zeta_m^2\pi a_m^2\kappa^2}{\nu\rho_d}\left[1 - \frac{2}{j\kappa a_m}\frac{J_1(j\kappa a_m)}{J_0(j\kappa a_m)} + \frac{J_1^2(j\kappa a_m)}{J_0^2(j\kappa a_m)}\right] + \pi a_m^2\lambda_m \quad (28d)$$

$$Q^*_{p,m}(0) = \pi a_m^2\frac{a_m^2}{8\nu\rho_d} \quad (28e)$$

$$Q^*_{E,m}(0) = -\frac{\epsilon\zeta_m\pi a_m^2}{\nu\rho_d}\left[1 + 2\frac{jJ_1(j\kappa a_m)}{\kappa a_m J_0(j\kappa a_m)}\right] = I^*_{p,m}(0) \quad (28f)$$

IV. Pressure and Electric Field Distribution

In this section, we will study the distribution of pressure and electric field of each layer. Because of the heterogeneity of multilayer membranes, each layer has its own parameters, including the following: pressure gradient, P^*_m; strength of electric field, $E^*_{z,m}$; zeta potential, ζ_m; radius of pore, a_m; porosity, η_m; number of pores, N_m; and thickness of membrane, l_m.

For each layer, $E^*_{z,m}$ and P^*_m are field quantities and uniform in every pores. $I^*_{p,m}$, $I^*_{E,m}$, $Q^*_{p,m}$, and $Q^*_{E,m}$ are additive. For the entire membrane, the total current and flow rate of one layer are the same as those of the other layers, because of the requirement of continuity. The total pressure and potential decreases of a multilayer membrane are simply the sum of each layer. Thus, we have the following relationships:

$$\frac{N_1}{N_m} = \frac{\eta_1}{\eta_m}\left(\frac{a_m^2}{a_1^2}\right) \quad (29)$$

Based on eqs 29−33, we can determine the relationship of the

$$Q_{total} = \mathrm{Re}[Q^*_{total}e^{j\omega t}] = \mathrm{Re}[N_m(Q^*_{p,m}(\omega)P^*_m(\omega) + Q^*_{E,m}(\omega)E^*_{z,m}(\omega))e^{j\omega t}] \quad (30)$$

$$I_{total} = \mathrm{Re}[I^*_{total}e^{j\omega t}] = \mathrm{Re}[N_m(I^*_{p,m}(\omega)P^*_m(\omega) + I^*_{E,m}(\omega)E^*_{z,m}(\omega))e^{j\omega t}] \quad (31)$$

$$\Delta p = \mathrm{Re}[P^*Le^{j\omega t}] = \mathrm{Re}[\sum_{m=1}^{N} P^*_m l_m e^{j\omega t}] \quad (32)$$

$$\Delta U = \mathrm{Re}[E^*_z Le^{j\omega t}] = \mathrm{Re}[\sum_{m=1}^{N} E^*_{z,m} l_m e^{j\omega t}] \quad (33)$$

pressure gradient P^* and strength of the electric field E^*_z between all layers. We will express these quantities as functions of the corresponding quantities of the first layer.

A. Streaming Potential (Pressure-Driven Flow). In the case of streaming potential, the total pressure gradient P^* is a known input. At equilibrium, eq 21 becomes

$$E^*_{z,m} = -\left(\frac{I^*_{p,m}}{I^*_{E,m}}\right)P^*_m \qquad (\text{for } m = 1, ..., N) \quad (34)$$

and the continuity of current is satisfied automatically. From eq 30, we have

$$N_m(Q^*_{p,m}(\omega)P^*_m(\omega) + Q^*_{E,m}E^*_{z,m}) = N_1(Q^*_{p,1}(\omega)P^*_1(\omega) + Q^*_{E,1}E^*_{z,1}) \quad (35)$$

Substituting eq 34 into eq 35, we find the relationship between the pressure gradient in the mth layer and that of the first layer to be

$$P^*_m = \frac{N_1}{N_m}\left[\frac{Q^*_{p,1} - \frac{(I^*_{p,1})^2}{Q^*_{E,1}}}{Q^*_{p,m} - \frac{(I^*_{p,m})^2}{I^*_{E,m}}}\right]P^*_1 \quad (36)$$

From eq 32, we have

$$P^*L = P^*_1\sum_{m=1}^{N} l_m\left(\frac{N_1}{N_m}\right)\left[\frac{Q^*_{p,1} - \frac{(I_{p,1})^2}{I_{E,1}}}{Q^*_{p,m} - \frac{(I_{p,m})^2}{I_{E,m}}}\right] \quad (37)$$

Using a known pressure gradient, one can solve for the pressure gradient of every layer. The total streaming potential (potential decrease) then is the sum of the potential decreases in each layer:

$$E_z^* = P^* \sum_{m=1}^{N} \left\{ -l_m \left(\frac{I_{p,m}^*}{I_{E,m}^*} \right) \left(\frac{N_1}{N_m} \right) \left[\frac{Q_{p,1}^* - \frac{(I_{p,1})^2}{I_{E,1}}}{Q_{p,m}^* - \frac{(I_{p,m})^2}{I_{E,m}}} \right] \times \left[\frac{1}{\sum_{m=1}^{N} l_m \left(\frac{N_1}{N_m} \right) \left[\frac{Q_{p,1}^* - \frac{(I_{p,1})^2}{I_{E,1}}}{Q_{p,m}^* - \frac{(I_{p,m})^2}{I_{E,m}}} \right]} \right] \right\} \quad (38)$$

B. Electro-osmosis (Electric-Field-Driven Flow). As for electro-osmosis, the known inputs are the total strength of the electric field and the pressure gradient. Normally, both ends of an electro-osmotic system are opened to the atmosphere, to eliminate the effect of hydrostatic pressure, so that $P^* = 0$. The continuities of current and flow rate can be expressed as

$$N_m(Q_{p,m}^*(\omega)P_m^*(\omega) + Q_{E,m}^* E_{z,m}^*) = N_1(Q_{p,1}^*(\omega)P_1^*(\omega) + Q_{E,1}^* E_{z,1}^*) \quad (39)$$

$$N_m(I_{p,m}^*(\omega)P_m^*(\omega) + I_{E,m}^* E_{z,m}^*) = N_1(I_{p,1}^*(\omega)P_1^*(\omega) + I_{E,1}^* E_{z,1}^*) \quad (40)$$

Note that, with $Q_{E,m}^* = I_{p,m}^*$, P_m^* and E_m^* can be solved from eqs 39 and 40:

$$P_m^* = \frac{N_1}{N_m}\left[\frac{I_{p,m}^* I_{p,1}^* - I_{E,m}^* Q_{p,1}^*}{(I_{p,m}^*)^2 - I_{E,m}^* Q_{p,m}^*}\right] P_1^* + \frac{N_1}{N_m}\left[\frac{I_{p,m}^* I_{E,1}^* - I_{E,m}^* I_{p,1}^*}{(I_{p,m}^*)^2 - I_{E,m}^* Q_{p,m}^*}\right] E_{z,1}^* \quad (41)$$

$$E_{z,m}^* = \frac{N_1}{N_m}\left[\frac{I_{p,m}^* Q_{p,1}^* - Q_{p,m}^* I_{p,1}^*}{(I_{p,m}^*)^2 - I_{E,m}^* Q_{p,m}^*}\right] P_1^* + \frac{N_1}{N_m}\left[\frac{I_{p,m}^* I_{p,1}^* - Q_{p,m}^* I_{E,1}^*}{(I_{p,m}^*)^2 - I_{E,m}^* Q_{p,m}^*}\right] E_{z,1}^* \quad (42)$$

Following eqs 32 and 33, we obtain the following set of equations:

$$P^* L = P_1^* \sum_{m=1}^{N} l_m \left(\frac{N_1}{N_m} \right) \left[\frac{I_{p,m}^* I_{p,1}^* - I_{E,m}^* Q_{p,1}^*}{(I_{p,m}^*)^2 - I_{E,m}^* Q_{p,m}^*} \right] + E_{z,1}^* \sum_{m=1}^{N} l_m \left(\frac{N_1}{N_m} \right) \left[\frac{I_{p,m}^* I_{E,1}^* - I_{E,m}^* I_{p,1}^*}{(I_{p,m}^*)^2 - I_{E,m}^* Q_{p,m}^*} \right] \quad (43)$$

$$E_z^* L = P_1^* \sum_{m=1}^{N} l_m \left(\frac{N_1}{N_m} \right) \left[\frac{I_{p,m}^* Q_{p,1}^* - Q_{p,m}^* I_{p,1}^*}{(I_{p,m}^*)^2 - I_{E,m}^* Q_{p,m}^*} \right] + E_{z,1}^* \sum_{m=1}^{N} l_m \left(\frac{N_1}{N_m} \right) \left[\frac{I_{p,m}^* I_{p,1}^* - Q_{p,m}^* I_{E,1}^*}{(I_{p,m}^*)^2 - I_{E,m}^* Q_{p,m}^*} \right] \quad (44)$$

For brevity, we write eqs 43 and 44, respectively, as

$$P^* L = A_{11} P_1^* + A_{12} E_{z,1}^* \quad (45)$$

$$E_z^* L = A_{21} P_1^* + A_{22} E_{z,1}^* \quad (46)$$

Solving these last two equations, we obtain

$$P_1^* = \frac{A_{22} L}{A_{11}A_{22} - A_{21}A_{12}} P^* - \frac{A_{12} L}{A_{11}A_{22} - A_{21}A_{12}} E_z^* \quad (47)$$

$$E_{z,1}^* = -\frac{A_{21} L}{A_{11}A_{22} - A_{21}A_{12}} P^* + \frac{A_{11} L}{A_{11}A_{22} - A_{21}A_{12}} E_z^* \quad (48)$$

Thus, $E_{z,m}^*$ and P_m^* could be determined from

$$P_m^* = \frac{N_1}{N_m}\left[\frac{I_{p,m}^* I_{p,1}^* - I_{E,m}^* Q_{p,1}^*}{(I_{p,m}^*)^2 - I_{E,m}^* Q_{p,m}^*}\right]\left[\left(\frac{A_{22} L}{A_{11}A_{22} - A_{21}A_{12}}\right) P^* - \left(\frac{A_{12} L}{A_{11}A_{22} - A_{21}A_{12}}\right) E_z^*\right] - \frac{N_1}{N_m}\left[\frac{I_{p,m}^* I_{E,1}^* - I_{E,m}^* I_{p,1}^*}{(I_{p,m}^*)^2 - I_{E,m}^* Q_{p,m}^*}\right] \times \left[\left(\frac{A_{21} L}{A_{11}A_{22} - A_{21}A_{12}}\right) P^* - \left(\frac{A_{11} L}{A_{11}A_{22} - A_{21}A_{12}}\right) E_z^*\right] \quad (49)$$

$$E_{z,m}^* = \frac{N_1}{N_m}\left[\frac{I_{p,m}^* Q^* {}_{p,1}^* - Q_{p,m}^* I_{E,1}^*}{(I_{p,m}^*)^2 - I_{E,m}^* Q_{p,m}^*}\right]\left[\left(\frac{A_{22} L}{A_{11}A_{22} - A_{21}A_{12}}\right) P^* - \left(\frac{A_{12} L}{A_{11}A_{22} - A_{21}A_{12}}\right) E_z^*\right] - \frac{N_1}{N_m}\left[\frac{I_{p,m}^* I_{p,1}^* - Q_{p,m}^* I_{E,1}^*}{(I_{p,m}^*)^2 - I_{E,m}^* Q_{p,m}^*}\right] \times \left[\left(\frac{A_{21} L}{A_{11}A_{22} - A_{21}A_{12}}\right) P^* - \left(\frac{A_{11} L}{A_{11}A_{22} - A_{21}A_{12}}\right) E_z^*\right] \quad (50)$$

If both sides of an electro-osmotic system are opened to the atmosphere, which implies $P^* = 0$, the value of P_m^* in eq 49 would be nonzero. Because of the heterogeneity of the multilayer membranes, pressure gradients are induced, as a result of current and flow-rate continuities. The expressions for the experimentally measurable total current (I_{total}) and flow rate (Q_{total}) are, respectively,

$$I_{\text{total}} = N_m(I_{p,m}^* P_m^* + I_{E,m}^* E_{z,m}^*) \quad (51)$$

$$Q_{\text{total}} = N_m(Q_{p,m}^* P_m^* + I_{p,m}^* E_{z,m}^*) \quad (52)$$

Note that N_m is measurable or calculable using the relation $N_m = \eta_m S/(\pi a_m^2)$, where S is the surface area of the multilayer membrane. For a typical electro-osmosis experimental system with $P^* = 0$, we can express the following equations:

$$I_{\text{total}} = N_1\left[\frac{(A_{11} I_{E,1}^* - A_{12} I_{p,1}^*)L}{A_{11}A_{22} - A_{21}A_{12}}\right] E_z^* \quad (53)$$

$$Q_{\text{total}} = N_1\left[\frac{(A_{11} I_{p,1}^* - A_{12} Q_{p,1}^*)L}{A_{11}A_{22} - A_{21}A_{12}}\right] E_z^* \quad (54)$$

$$\frac{Q_{\text{total}}}{I_{\text{total}}} = \frac{A_{11} I_{p,1}^* - A_{12} Q_{p,1}^*}{A_{11} I_{E,1}^* - A_{12} I_{p,1}^*} \quad (55)$$

Equation 55 is a complex function of the frequency ω, which includes all the information of each layer, such as zeta potential, thickness, porosity, and pore size.

TABLE 1: Physical and Chemical Properties of the Multilayer Membrane

	support layer (layer 1)	intermediate layer (layer 2)	skin layer (layer 3)
thickness (mm)	1	0.5	0.1
mean pore size (μm)	10	1	0.1
porosity (%)	30	25	20

TABLE 2: Frequency-Dependent Electric-Field Strength on the Streaming Potentials for a Three-Layer Multilayer Membrane[a]

ω (rad/s)	E_z^* (V/m)	$\lvert E_z^*\rvert$ (V/m)	phase angle of E_z^*, ϕ (degrees)
5×10^1	$-4.35432 + 3.24187 \times 10^{-6}j$	4.35432	180
5×10^3	$-4.35432 + 0.00032421j$	4.35432	179.996
5×10^6	$-4.32576 + 0.0341881j$	4.33945	175.481

[a] For zeta potentials of $\zeta_1 = -100$ mV, $\zeta_2 = -50$ mV, and $\zeta_3 = -75$ mV.

As an example, a typical three-layer membrane is considered with the parameters shown in Table 1. For a parametric study, we consider the following parameters: $\epsilon = 7.0832 \times 10^{-10}$ C/(V m), $\rho = 1 \times 10^3$ kg/m^3, $\mu = 0.9 \times 10^{-3}$ kg/(m s), $\upsilon = 0.9 \times 10^{-6}$ m^2/s, $e = 1.6021 \times 10^{-19}$ Coulomb, $k = 1.3805 \times 10^{-23}$ J/(mol K) and $T = 298$ K. We have chosen a 0.1 M KCl solution as the testing liquid, with a conductivity of $\lambda = 1.28217$ S/m.[30]

C. Pressure and Electric Field under Streaming Potential. Assuming a total pressure gradient P^* of 10^8 Pa/m and zeta potentials of $\zeta_1 = -100$ mV, $\zeta_2 = -50$ mV, and $\zeta_3 = -75$ mV, we calculate the complex streaming potentials for ω values of 5×10^1, 5×10^3, and 5×10^6 rad/s; the results are shown in Table 2. We see that, when the input frequency changes from 5×10^1 rad/s to 5×10^6 rad/s, the total streaming potential changes slightly. This implies that a traditional (steady-state) model can be used to determine the streaming potential using only the amplitudes of the properties, even when a high-frequency oscillation pressure is used. We note that if the difference in amplitude and phase angle can be detected, one can solve the set of equations for all the unknown parameters. Because the zeta potential is the most important chemical property of a membrane, here we study how the zeta potential of each layer affects the streaming potential, pressure, and electric-field distribution for different frequencies. In Table 3, we list the pressure gradient and electric-field strength in each layer of a three-layer membrane for $\omega = 0$ rad/s. Note that, when the zeta potentials of each layer are interchanged, the pressure gradient and electric field would be different. In this case, when the zeta potential of each layer interchanges, the pressure changes slightly but not the electric-field distribution. From this specific example, we obtained a larger streaming potential when $\zeta_3 = -100$ mV, which suggests that the skin layer (layer 3) significantly controls the electrokinetic property of this multilayer membrane. In Table 4, for $\omega = 10^7$ rad/s, we only list the amplitudes of the pressure gradient and electric-field strength in each layer, because the pressure gradient and electric-field strength change with time in this case. We can observe that the corresponding amplitudes of the electric-field strength ($\lvert E_z^*\rvert$) decrease as the frequency increases, up to $\omega = 10^7$ rad/s. This phenomenon, in an individual microchannel, has been studied elsewhere.[31,32] The difference in the zeta potential ζ of each layer could cause different output and electric-field strength E_z^*, which further implies a method to determine the properties of multilayer membranes by means of an oscillating streaming potential.

D. Pressure and Electric Field under Electro-osmosis. Assuming $P^* = 0$ (this is true for most electro-osmosis experiments), $E_z^* = 10^5$ V/m, $\zeta_1 = -100$ mV, $\zeta_2 = -50$ mV, and $\zeta_3 = -75$ mV, we can calculate the complex Q_{total}/I_{total} from eq 55 for $\omega = 5 \times 10^1$, 5×10^3, and 5×10^6 rad/s; the results are shown in Table 5. Because electro-osmosis is often used to measure the zeta potential, polarization of the electrodes and/or concentration polarization on the membrane surface can become the major influencing factor of experimental error.[22,33] Experience has shown that the effective way to prevent electrodes from polarizing is to use an alternating electric field as input. A traditional (steady-state) formula is often used to calculate the zeta potential, as in refs 22 and 33. From Table 5, we find that frequency is not a strong function of the amplitudes for the properties in consideration. Thus, a steady-state formula can be used, in principle.

Normally, electro-osmotic experiments are opened to the atmosphere for a hydrostatic equilibrium. However, because of the heterogeneity of the multilayer membrane, a pressure gradient is induced to maintain the current and flow-rate continuities. In Table 6, we study the pressure and electric-field distribution of a multilayer membrane for $\omega = 0$ rad/s and find that such a pressure gradient can be as high as 10^8 Pa/m.

Table 6 shows that, when the zeta potential of each layer interchanges, the pressure gradient and electric field will change. When the zeta potential of each layer interchanges, the electric field changes slightly but not the pressure distribution. From the results in this specific example, a larger ratio of flow rate to current is obtained when $\zeta_3 = -100$ mV, which suggests that the property of the skin layer dominates the electrokinetic feature of the multilayer membrane and the support layer has

TABLE 3: Pressure Gradient (P^*) and Electric-Field Strength (E_z^*) for a Three-Layer Multilayer Membrane with $P^* = 10^8$ Pa/m and $\omega = 0$ rad/s

	Layer 1		Layer 2		Layer 3		
	P_1^* (Pa/m)	$E_{z,1}^*$(V/m)	P_2^* (Pa/m)	$E_{z,2}^*$ (V/m)	P_3^* (Pa/m)	$E_{z,3}^*$ (V/m)	E_z^* (V/m)
$\zeta_1 = -100$ mV, $\zeta_2 = -50$ mV, $\zeta_3 = -75$ mV	102318	-0.6276×10^{-2}	1.2278×10^7	-0.3757	1.5376×10^9	-67.7	-4.35432
$\zeta_1 = -100$ mV, $\zeta_2 = -75$ mV, $\zeta_3 = -50$ mV	102417	-0.628×10^{-2}	1.229×10^7	-0.5633	1.53752×10^9	-45.77	-3.04051
$\zeta_1 = -50$ mV, $\zeta_2 = -100$ mV, $\zeta_3 = -75$ mV	102317	-0.3139×10^{-2}	1.2279×10^7	-0.7489	1.5376×10^9	-67.73	-4.46897
$\zeta_1 = -50$ mV, $\zeta_2 = -75$ mV, $\zeta_3 = -100$ mV	102183	-0.3135×10^{-2}	1.226×10^7	-0.562	1.5377×10^9	-88.63	-5.717
$\zeta_1 = -75$ mV, $\zeta_2 = -50$ mV, $\zeta_3 = -100$ mV	102183	-0.47×10^{-2}	1.226×10^7	-0.375	1.5377×10^9	-88.63	-5.6596
$\zeta_1 = -75$ mV, $\zeta_2 = -100$ mV, $\zeta_3 = -50$ mV	102417	-0.4713×10^{-2}	1.229×10^7	-0.7544	1.5375×10^9	-45.769	-3.0978

TABLE 4: Amplitudes of the Pressure Gradient (P^*) and Electric-Field Strength (E_z^*) for Three-Layer Multilayer Membranes with $P^* = 10^8$ Pa/m and $\omega = 10^7$ rad/s

	Layer 1		Layer 2		Layer 3		
	$\lvert P_1^*\rvert$ (Pa/m)	$\lvert E_{z,1}^*\rvert$ (V/m)	$\lvert P_2^*\rvert$ (Pa/m)	$\lvert E_{z,2}^*\rvert$ (V/m)	$\lvert P_3^*\rvert$ (Pa/m)	$\lvert E_{z,3}^*\rvert$ (V/m)	$\lvert E_z^*\rvert$ (V/m)
$\zeta_1 = -100$ mV, $\zeta_2 = -50$ mV, $\zeta_3 = -75$ mV	1.44939×10^7	0.0526701	2.54622×10^7	0.43101	1.50336×10^9	66.21	4.28856
$\zeta_1 = -100$ mV, $\zeta_2 = -75$ mV, $\zeta_3 = -50$ mV	1.45074×10^7	0.0527194	2.54862×10^7	0.646225	1.50325×10^9	44.7414	3.0105
$\zeta_1 = -50$ mV, $\zeta_2 = -100$ mV, $\zeta_3 = -75$ mV	1.44939×10^7	0.0263438	2.54626×10^7	0.859164	1.50336×10^9	66.2096	4.40208
$\zeta_1 = -50$ mV, $\zeta_2 = -75$ mV, $\zeta_3 = -100$ mV	1.44755×10^7	0.0263104	2.54299×10^7	0.644802	1.50351×10^9	86.6482	5.61627
$\zeta_1 = -75$ mV, $\zeta_2 = -50$ mV, $\zeta_3 = -100$ mV	1.44755×10^7	0.0394601	2.54299×10^7	0.430463	1.50351×10^9	86.6483	5.55955
$\zeta_1 = -75$ mV, $\zeta_2 = -100$ mV, $\zeta_3 = -50$ mV	1.45074×10^7	0.0395472	2.54864×10^7	0.859968	1.50325×10^9	44.7414	3.06739

TABLE 5: Frequency-Dependent Q_{Total}/I_{Total} for a Three-Layer Multilayer Membrane with Zeta Potentials of $\zeta_1 = -100$ mV, $\zeta_2 = -50$ mV, and $\zeta_3 = -75$ mV

ω (rad/s)	Q_{total}/I_{total} (m^3/(s A))	$\lvert Q_{total}/I_{total}\rvert$ (m^3/(s A))	phase angle of (Q_{total}/I_{total}) (degrees)
5×10^1	$4.35432 \times 10^{-8} - 3.24187 \times 10^{-14}j$	4.35432×10^{-8}	-0.0000426578
5×10^3	$4.35432 \times 10^{-8} - 3.24207 \times 10^{-12}j$	4.35432×10^{-8}	-0.004266
5×10^6	$4.32596 \times 10^{-8} - 3.41881 \times 10^{-9}j$	4.33945×10^{-8}	-4.5187

TABLE 6: Pressure Gradient (P^*) and Electric-Field Strength (E_z^*) in Three-Layer Multilayer Membranes with $P^* = 0$, $E_z^* = 10^5$ V/m, and $\omega = 0$ rad/s

	Layer 1		Layer 2		Layer 3		(Q_{total}/I_{total}) (m^3/(s A))
	P_1^* (Pa/m)	$E_{z,1}^*$ (V/m)	P_2^* (Pa/m)	$E_{z,2}^*$ (V/m)	P_3^* (Pa/m)	$E_{z,3}^*$ (V/m)	
$\zeta_1 = -100$ mV, $\zeta_2 = -50$ mV, $\zeta_3 = -75$ mV	-150644	91637	1.31481×10^7	109891	-6.4234×10^7	134174	4.35432×10^{-8}
$\zeta_1 = -100$ mV, $\zeta_2 = -75$ mV, $\zeta_3 = -50$ mV	-261661	91576	-1.5657×10^7	109665	8.09×10^7	135916	3.04051×10^{-8}
$\zeta_1 = -50$ mV, $\zeta_2 = -100$ mV, $\zeta_3 = -75$ mV	118669	91755.6	-1.657×10^7	109630	8.167×10^7	134295	4.46897×10^{-8}
$\zeta_1 = -50$ mV, $\zeta_2 = -75$ mV, $\zeta_3 = -100$ mV	224597	91837.5	1.15368×10^7	109940	-5.993×10^7	131925	5.71702×10^{-8}
$\zeta_1 = -75$ mV, $\zeta_2 = -50$ mV, $\zeta_3 = -100$ mV	89673.9	91788	2.64432×10^7	110049	-1.33813×10^8	131876	5.65962×10^{-8}
$\zeta_1 = -75$ mV, $\zeta_2 = -100$ mV, $\zeta_3 = -50$ mV	-127262	91644.5	-3.05×10^7	109513	1.53665×10^8	135989	3.09775×10^{-8}

TABLE 7: Amplitudes of the Pressure Gradient (P^*) and the Electric-Field Strength (E_z^*) for Three-Layer Multilayer Membranes with $P^* = 0$, $E_z^* = 10^5$ V/m, and $\omega = 10^7$ rad/s

	Layer 1		Layer 2		Layer 3		$\lvert(Q_{total}/I_{total})\rvert$ (m^3/(s A))
	$\lvert P_1^*\rvert$ (Pa/m)	$\lvert E_{z,1}^*\rvert$ (V/m)	$\lvert P_2^*\rvert$ (Pa/m)	$\lvert E_{z,2}^*\rvert$ (V/m)	$\lvert P_3^*\rvert$ (Pa/m)	$\lvert E_{z,3}^*\rvert$ (V/m)	
$\zeta_1 = -100$ mV, $\zeta_2 = -50$ mV, $\zeta_3 = -75$ mV	4.90382×10^7	91637	6.29079×10^7	109890	7.98017×10^8	134179	4.28856×10^{-8}
$\zeta_1 = -100$ mV, $\zeta_2 = -75$ mV, $\zeta_3 = -50$ mV	3.34169×10^7	91575.8	3.2047×10^7	109665	4.84826×10^8	135918	3.0105×10^{-8}
$\zeta_1 = -50$ mV, $\zeta_2 = -100$ mV, $\zeta_3 = -75$ mV	5.22506×10^7	91755.3	4.73842×10^7	109629	7.50951×10^8	134301	4.40208×10^{-8}
$\zeta_1 = -50$ mV, $\zeta_2 = -75$ mV, $\zeta_3 = -100$ mV	6.71992×10^7	91836.8	7.77547×10^7	109939	1.05708×10^9	131936	5.61627×10^{-8}
$\zeta_1 = -75$ mV, $\zeta_2 = -50$ mV, $\zeta_3 = -100$ mV	6.55771×10^7	91787.1	8.95546×10^7	110048	1.08891×10^9	131888	5.55955×10^{-8}
$\zeta_1 = -75$ mV, $\zeta_2 = -100$ mV, $\zeta_3 = -50$ mV	3.49921×10^7	91644.4	3.63542×10^7	109513	4.81058×10^8	135991	3.06739×10^{-8}

less influence on the total electrokinetic flow. For $\omega = 10^7$ rad/s, we only list the amplitudes of the pressure gradient and electric-field strength in each layer in Table 7, because the pressure gradient and electric-field strength change with time in this case. We can find that the corresponding amplitudes of the ratio of flow rate to current (Q_{total}/I_{total}) decrease as the frequency increases, up to $\omega = 10^7$ rad/s. Tables 2−7 show that the values of E_z^* are the same as those of Q_{total}/I_{total}, implying that the total quantities of a multilayer membrane also satisfy the well-known Onsager's principle of reciprocity.[29]

The traditional method to measure the zeta potential collects only a set of limited data: the streaming potential, streaming current, and flow rate can be measured by pressure-driven flow (pressure is an input), whereas electro-osmotic current and flow rate can be measured by electric-field-driven flow (electric field is an input and the pressure decrease is zero). Because the pressure gradient and strength of electric field are respectively proportional to the measured quantities in pressure-driven-flow and electric-field-driven flow, one cannot change the pressure gradient and the electric-field strength directly to obtain more

independent equations. Since eq 55 is a complex function of frequency and can be reduced to the form of eq 15, each measurement provides two equations from the amplitude and phase angle of eq 15. Two equations are not sufficient to determine all the details of a multilayer membrane. If one can measure the minor differences (amplitude or phase angle) of any given quantities in terms of frequencies, all the information of a multilayer membrane can be determined. This is made possible by providing more equations to determine all parameters in multilayer membranes. This method might be a potential application to determine the properties of an unknown multilayer membrane, including the thickness, pore size, and zeta potentials of each layer.

V. Conclusions

A model of oscillating electrokinetic flow through multilayer membranes has been developed. The cases for pressure-driven flow (streaming potential) and electric-field-driven flow (electroosmosis) have been studied. According to our solutions, pressure and electric-field distributions in each layer can be obtained by means of an oscillating frequency. Knowledge of the pressure and electric-field distributions benefits the design and selection of artificial membranes. Our model also predicts a nonuniform induced electric field (pressure-driven flow) and pressure distributions that are due to current and flow-rate continuities. Because the complex response of an oscillating input provides more information of each layer than that of steady state, a potential approach to determine the electrokinetic properties (such as zeta potential) and physical properties of each layer through the use of an alternating input is proposed.

Acknowledgment. D.Y.K. gratefully acknowledges financial support from the Alberta Ingenuity Establishment Fund, the Canada Research Chair (CRC) Program, the Canada Foundation for Innovation (CFI), and the Natural Sciences and Engineering Research Council of Canada (NSERC) in partial support of this research. J.Y. acknowledges financial support from a Studentship Award by the Alberta Ingenuity Fund in the Province of Alberta.

References and Notes

(1) Szymczyk, A.; Fievet, P.; Reggiani, J. C.; Pagetti, J. *J. Membr. Sci.* **1998**, *146*, 277−284.

(2) Fane, J. K. K. A. G.; Nystrom, M.; Pihlajamaki, A.; Bowen, W. R.; Mukhtar, H. *J. Membr. Sci.* **1996**, *116*, 149−159.

(3) Pontié, M.; Chasseray, X.; Lemordant, D.; Lainé, J. M. *J. Membr. Sci.* **1997**, *129*, 125−133.

(4) Möckel, D.; Staude, E.; Dal-Cin, M.; Darcovich, K.; Guiver, M. *J. Membr. Sci.* **1998**, *145*, 221.

(5) Ibañez, J. A.; Forte, J.; Hernandez, A.; Tejerina, F. *J. Membr. Sci.* **1988**, *36*, 45.

(6) Fievet, P.; Szymczyk, A.; Labbez, C.; Aoubiza, B.; Simon, Y. C.; Foissy, Z. A.; Pagett, J. *J. Colloid Interface Sci.* **2001**, *235*, 383−390.

(7) Koh, W.; Anderson, J. L. *AIChE J.* **1975**, *21*, 1176.

(8) Lee, C. K.; Hong, J. *J. Membr. Sci.* **1988**, *39*, 79.

(9) Bowen, W. R.; Mukhtar, H. *Colloids Surf. A* **1993**, *81*, 93.

(10) Vernhet, A.; Bellon-Fontaine, M. N.; Doren, A. *J. Chim. Phys.* **1994**, *91*, 1728.

(11) Mullet, M.; Fievet, P.; Reggiani, J. C.; Pagetti, J. *J. Membr. Sci.* **1997**, *123*, 255.

(12) Greberg, H.; Kjellander, R. *J. Chem. Phys.* **1998**, *108*, 2940.

(13) González-Tovar, E.; Lozada-Cassou, M.; Olivares, W. *J. Chem. Phys* **1991**, *94*, 2219.

(14) Olivares, W.; Sulbarán, B.; Lozada-Cassou, M. *J. Phys. Chem.* **1993**, *97*, 4780.

(15) Olivares, W.; Sulbarán, B.; Lozada-Cassou, M. *J. Chem. Phys.* **1995**, *103*, 8179.

(16) Zaini, P.; Modarress, H.; Mansoori, G. A. *J. Chem. Phys.* **1996**, *104*, 3832.

(17) Lykema, J., Ed. *Fundamentals of Interface and Colloid Science*; Academic Press: New York, 1995; Vol. II.

(18) Yang, J.; Kwok, D. Y. *J. Phys. Chem. B* **2002**, *106*, 12851−12855.

(19) Yang, J.; Kwok, D. Y. *J. Chem. Phys.* **2003**, *118*, 354−363.

(20) Szymczyk, A.; Fievet, P.; Reggiani, J. C.; Pagetti, J. *Desalination* **1998**, *116*, 81−88.

(21) Szymczyk, A.; Labbez, C.; Fievet, P.; Aoubiza, B.; Simon, C. *AICHE J* **2001**, *47*, 2349−2358.

(22) Wang, J.; Liu, Z.; He, Q. H.; Ding, F. X.; Yuan, N. J. *Separ. Sci. Technol.* **2000**, *35*, 1195−1206.

(23) Masliyah, J. H. *Electrokinetic Transport Phenomena*; Alberta Oil Sands Technology and Research Authority: Edmonton, Alberta, Canada, 1994.

(24) Shadowitz, A. *The Electromagnetic Field*; Dover Publications: New York, 1975.

(25) Hunter, R. J. *Introduction to Modern Colloid Science*; Oxford University Press: New York, 1993.

(26) Bowen, W. R.; Jenner, F. *J. Colloid Interface Sci.* **1995**, *173*, 388−395.

(27) Bowen, W. R.; Cao, X. W. *J. Membr. Sci.* **1998**, *140*, 267−273.

(28) Schimd, G. *J. Membr. Sci.* **1998**, *150*, 151−157.

(29) Rice, C. L.; Whitehead, R. *J. Phys. Chem.* **1965**, *69*, 4017−4024.

(30) Newman, J. S. *Electrochemical Systems, 2nd Ed.*; Prentice Hall: Englewood Cliffs, NJ, 1991.

(31) Bhattacharyya, A.; Masliyah, J. H.; Yang, J. *J. Colloid Interface Sci.* **2003**, *261*, 12−20.

(32) Yang, J.; Bhattacharyya, A.; Masliyah, J. H.; Kwok, D. Y. *J. Colloid Interface Sci.* **2003**, *261*, 21−31.

(33) Liu, Z.; Yang, H.; Huang, Z.; Wang, J.; Ding, F. X.; Yuan, N. J. *Separ. Sci. Technol.* **1996**, *31*, 2257−2271.